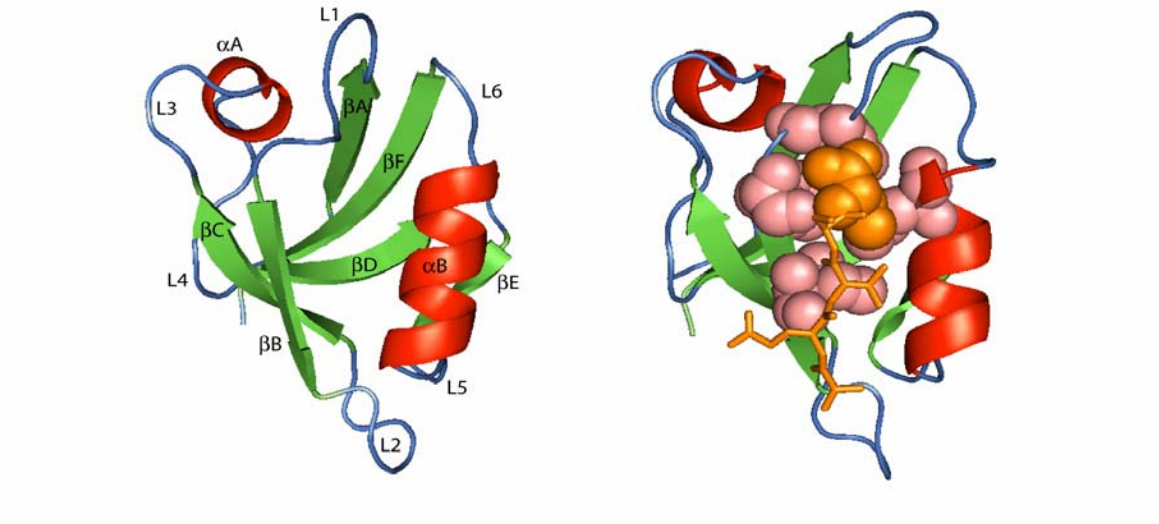

Figure 1. Cartoon representation of the X-ray structure of the PDZ3 domain of PSD-95 without (left) and with (right) bound peptide. Secondary structures are highlighted by different colors: red for α-helices, green for β-strands and blue for loops, and they are labeled in accordance with…. The bound peptide (orange, right figure) is shown in stick representation, apart from the C-terminal valine, all the atoms of whom are shown to emphasize that it sits in a hydrophobic pocket lined by Leu-323, Phe-325, Ile-327 and Leu-379 (pink all-atom representation, right figure).

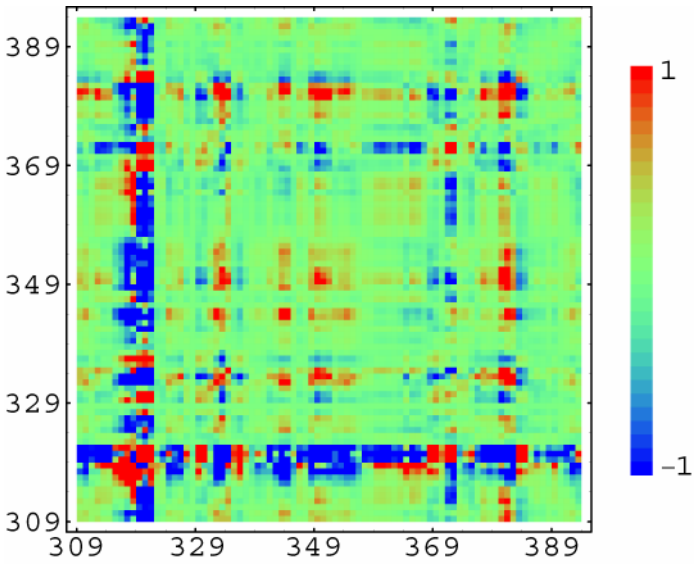

Figure 2. Internal Cα-Cα correlations of the distortion induced by the binding for the PDZ3 domain of PSD-95, computed according to equation 1. Red (blue) regions correspond to (anti)parallel distortions. The loop L1 and helix αB are the most mobile regions of the protein, and they are mutually antiparallel. The loop L1 displacement is actually antiparallel to most other elements of the protein.

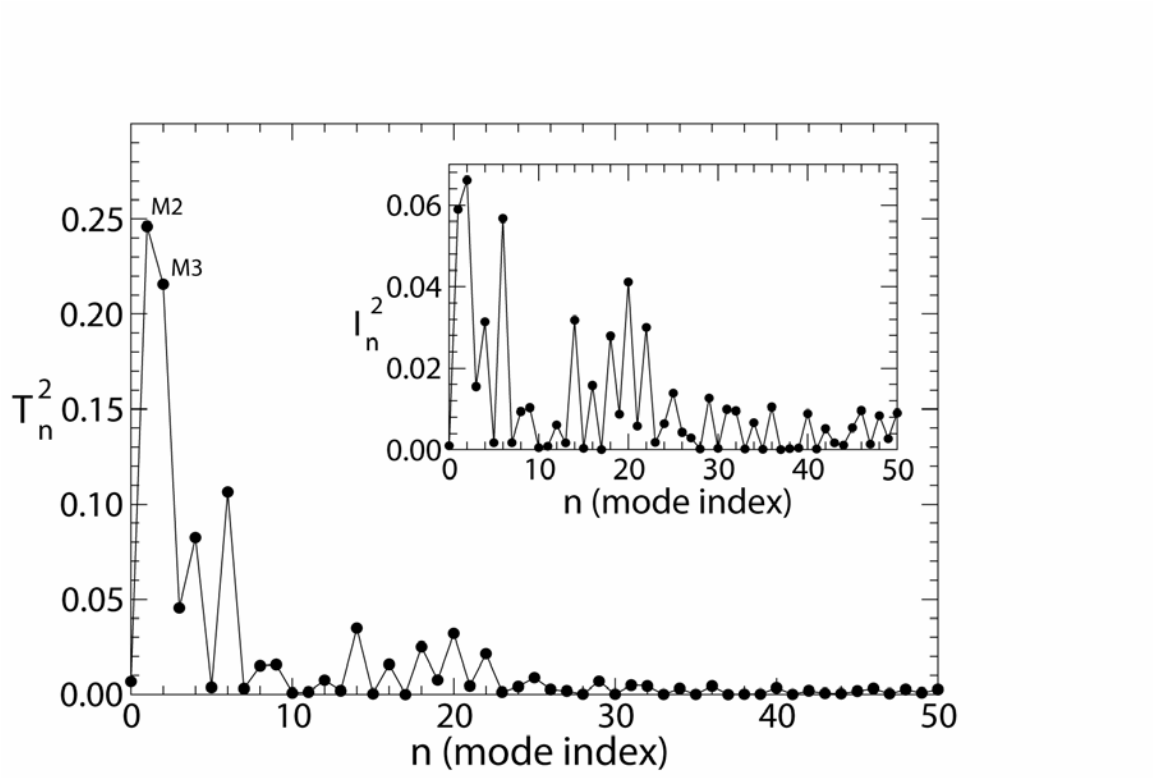

Figure 3. The thermodynamic involvement coefficients T_n of the Charmm modes of the PDZ3 domain of PSD-95. We plot the squares of the coefficients so that they have unitary sum, and the displayed values represent their percentage contributions to the thermodynamic fluctuations of the overlap between the binding deformation and a thermodynamic structure fluctuations (equation 8). Inset: the usual involvement coefficients I_n (equation 7).

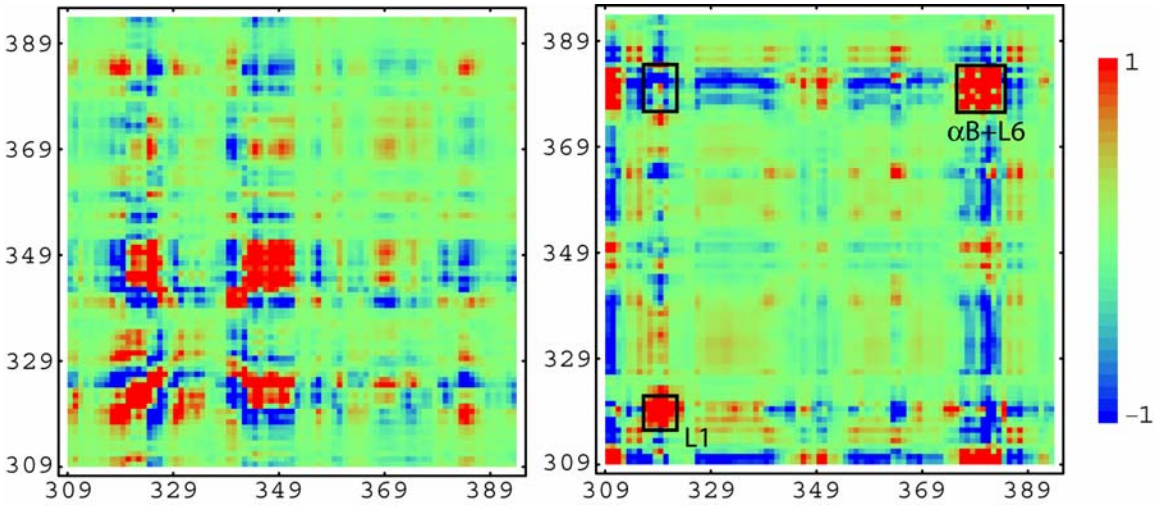

Figure 4. Internal Cα-Cα correlations for M2 (left) and M3 (right) Charmm vibrational normal modes of the PDZ3 domain of PSD-95. M3 (right) shows a pattern rather similar to the internal correlations of the binding distortion (Figure 2).

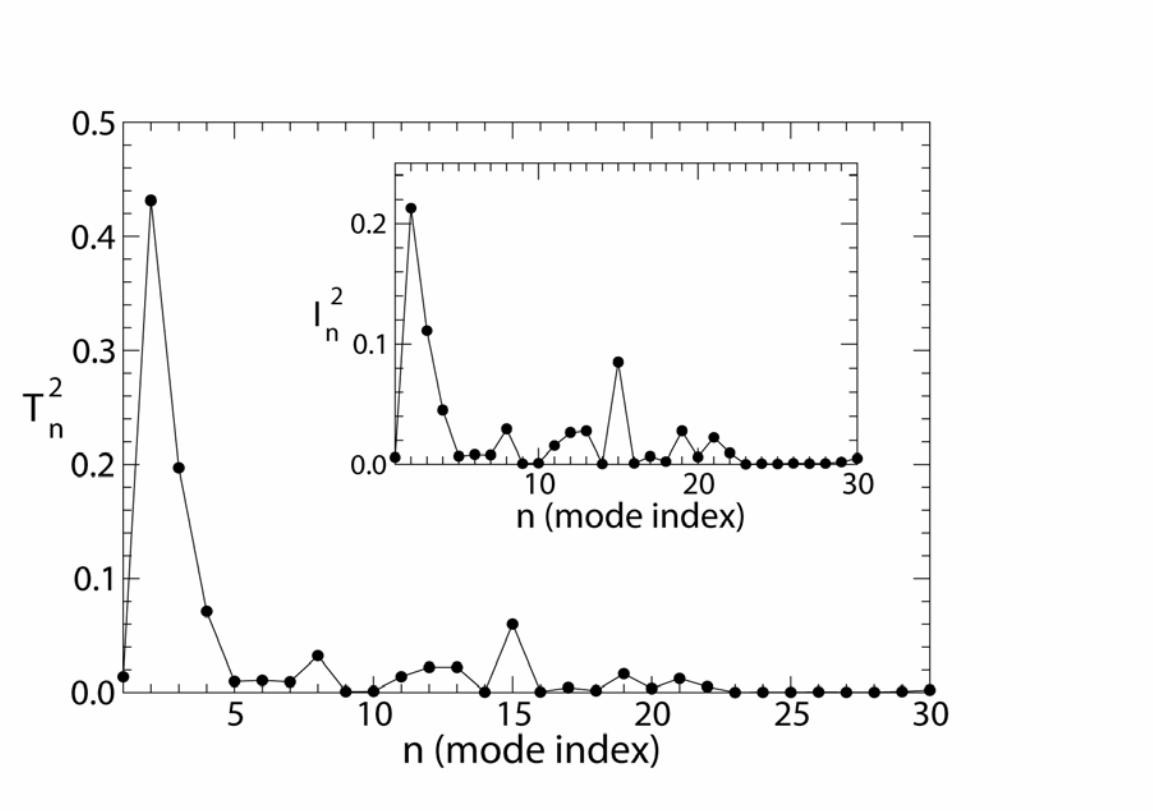

Figure 5. The thermodynamic involvement coefficients T_n of the Cβ-ANM modes of the PDZ3 domain of PSD-95. We plot the squares of the coefficients so that they have unitary sum, and the displayed values represent their percentage contributions to the thermodynamic fluctuation of the overlap between the binding deformation and a thermodynamic structure fluctuation (equation 8). Inset: the usual involvement coefficients I_n (equation 7).

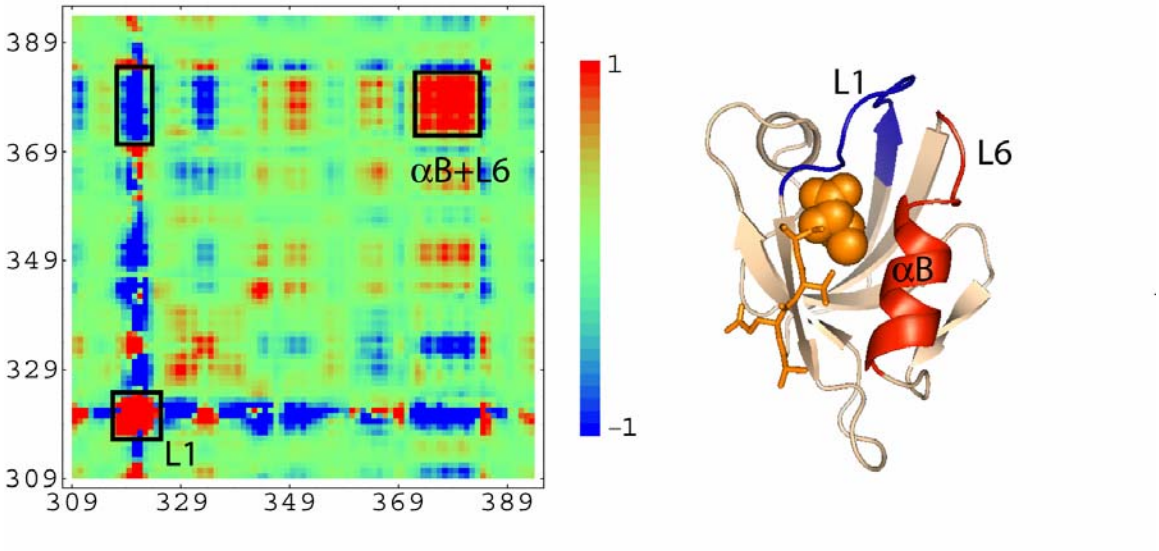

Figure 6. (Right) Internal Cα-Cα correlations for the second Cβ-ANM normal mode of the PDZ3 domain of PSD-95. They are remarkably similar to the internal correlations of the binding deformation. (Right) The regions most affected by the displacements are represented in blue (loop L1) and red (helix αB), with the peptide shown in orange.

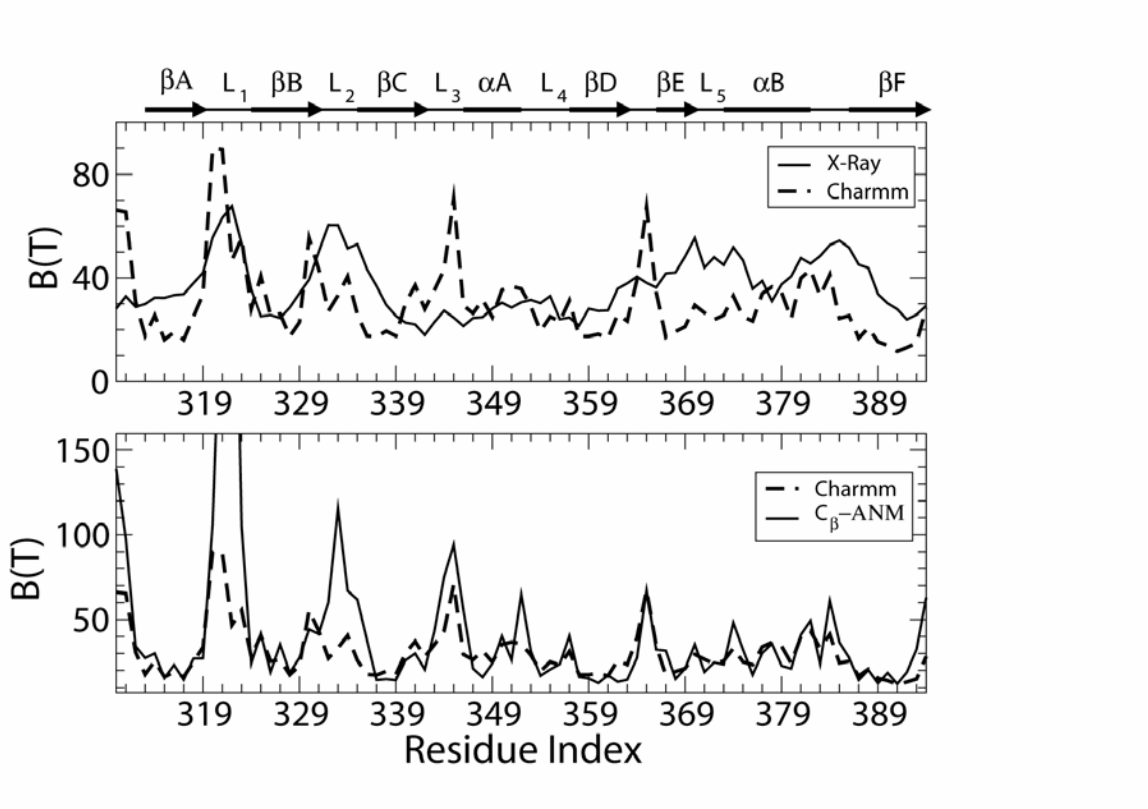

Figure 7. Comparison of experimental (X-ray) and theoretical (Charmm and Cβ-ANM) B-factors of the PDZ3 domain. Whereas the Charmm and Cβ-ANM B-factors show a very remarkable mutual agreement (lower panel), they are much less in agreement with the X-ray ones. B-factors are expressed in $Å^2$.

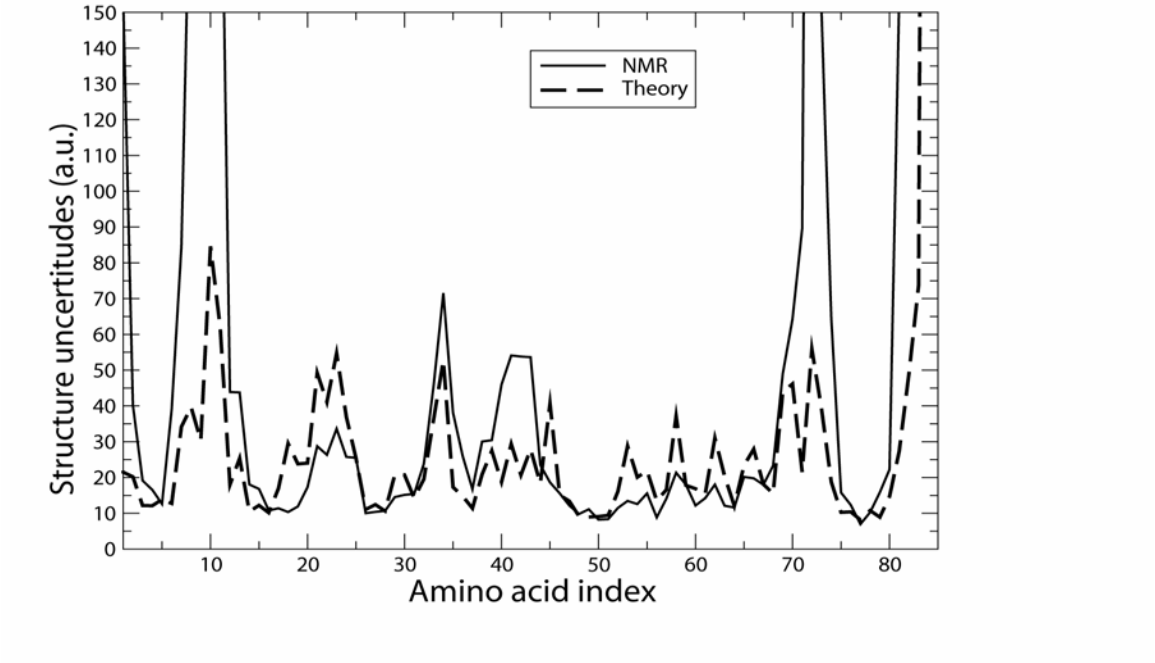
NMR
Theory
Structure uncertitudes (a.u.)
Amino acid index
0
10
20
30
40
50
60
70
80
90
100
110
120
130
140
150

Figure 8

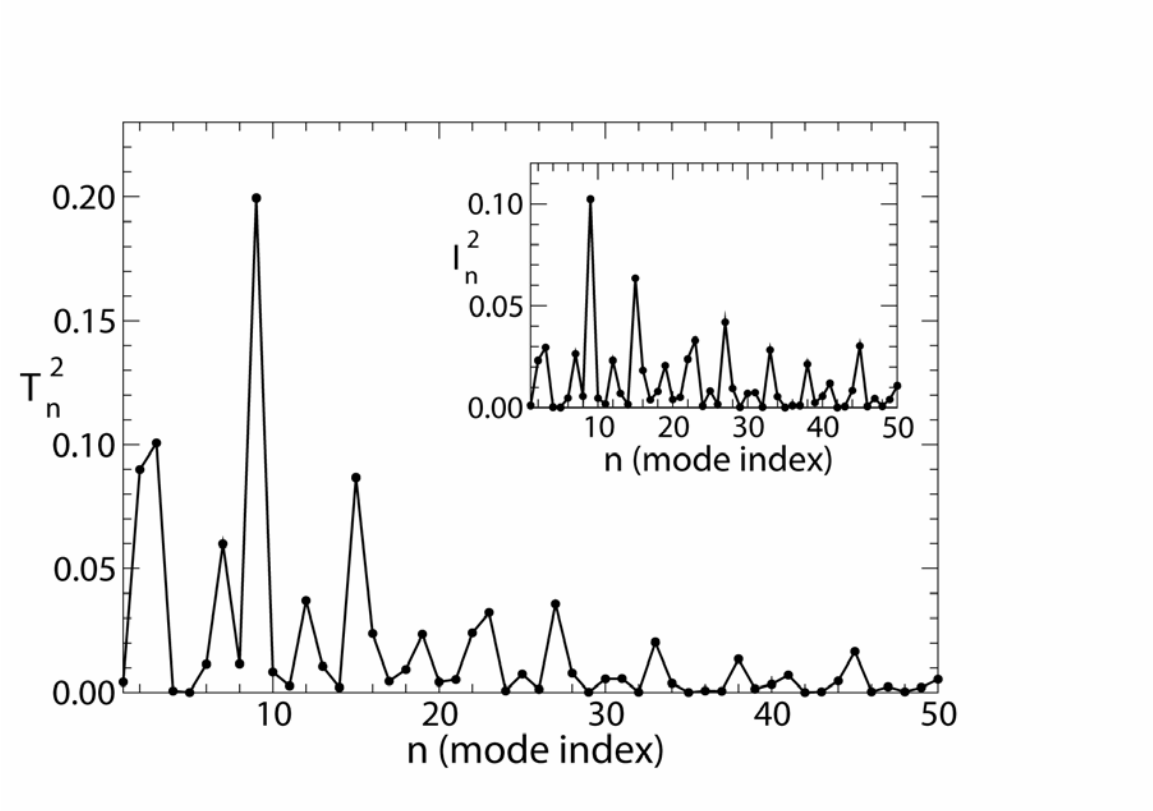

Figure 9. The thermodynamic involvement coefficients T_n of the Cβ-ANM modes of the PDZ2 domain of hPTP1E. We plot the squares of the coefficients so that they have unitary sum, and the displayed values represent their percentage contributions to the thermodynamic fluctuation of the overlap between the binding deformation and a thermodynamic structure fluctuation (equation 8). Inset: the usual involvement coefficients I_n (equation 7).

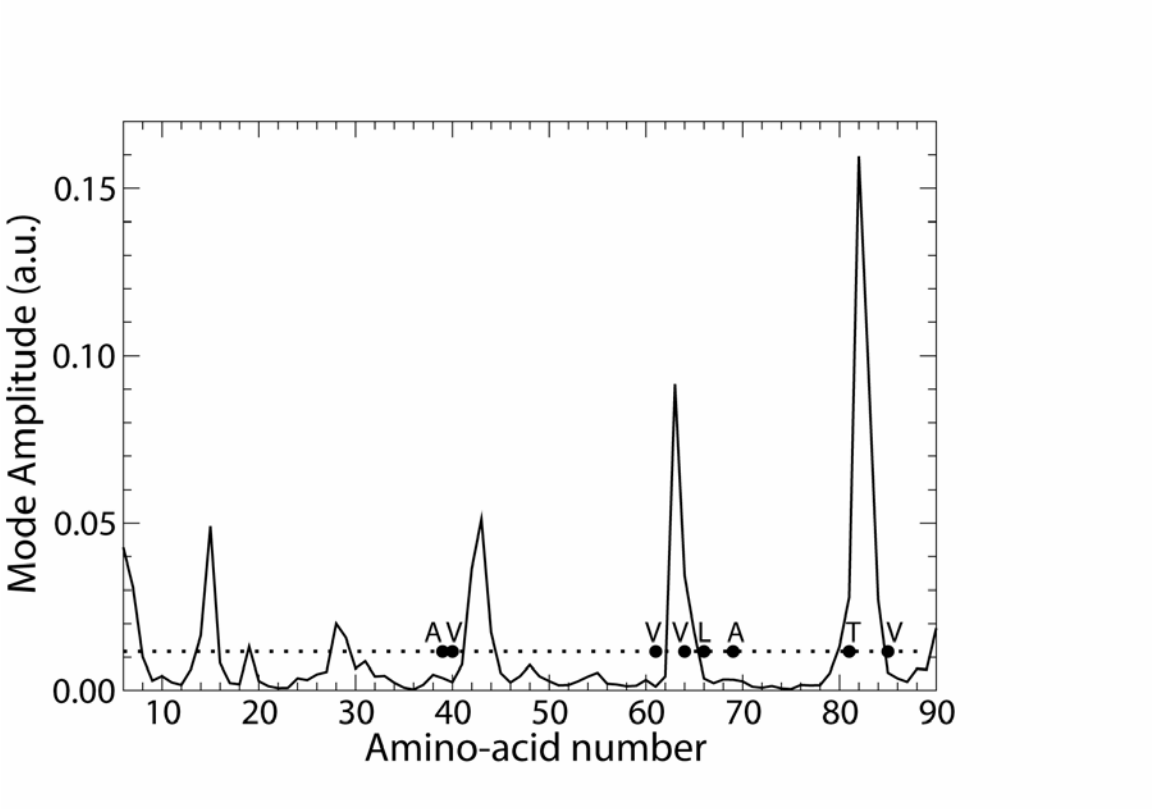

Figure 10. Square fluctuation amplitudes of the ninth Cβ-ANM normal mode of the PDZ2 domain of hPTP1E. The dotted line is the average square displacement. The circles mark the amino-acids that are dynamically most affected by the binding process, and they are labeled by their amino-acid species (1-letter code for clarity).